Journal of Computational and Applied Mathematics 361 (2019) 459–471

Contents lists available at ScienceDirect

Journal of Computational and Applied Mathematics

journal homepage: www.elsevier.com/locate/cam

A *priori* error analysis for transient problems using Enhanced Velocity approach in the discrete-time setting

Yerlan Amanbek [a,b,*], Mary F. Wheeler [a]

[a] *Center for Subsurface Modeling, Oden Institute for Computational Engineering and Sciences, University of Texas at Austin, 201 East 24th St, Stop C0200, POB 4.102, Austin, TX, USA*
[b] *Nazarbayev University, Kabanbay Batyr Avenue 53, Astana, Kazakhstan*

ARTICLE INFO

Article history:
Received 12 December 2018
Received in revised form 24 March 2019

Keywords:
A priori error analysis
Enhanced velocity
Mixed finite element method
Error estimates
Darcy flow

ABSTRACT

Time discretization along with space discretization is important in the numerical simulation of subsurface flow applications for long run. In this paper, we derive theoretical convergence error estimates in discrete-time setting for transient problems with the Dirichlet boundary condition. Enhanced Velocity Mixed FEM as domain decomposition method is used in the space discretization and the backward Euler method and the Crank–Nicolson method are considered in the discrete-time setting. Enhanced Velocity scheme was used in the adaptive mesh refinement dealing with heterogeneous porous media [1,2] for single phase flow and transport and demonstrated as mass conservative and efficient method. Numerical tests validating the backward Euler theory are presented. These error estimates are useful in the determining of time step size and the space discretization size.

1. Introduction

The most subsurface flow equations are dynamic and time-dependent problems. In decision making process, numerical simulation of flow plays vital role in many engineering applications such as oil and gas production evaluation, CO_2 sequestration and contaminate transport problems. It is natural to deal with non-matching multiblock grids in the reservoir simulation since subsurface parameters such as permeability or porosity can vary over subdomains substantially. The accuracy of simulation can depend on discretization method of space and time variables. For space discretization, we are concerned with a well-established domain decomposition method, i.e. Enhanced Velocity Mixed Finite Element Method (EVMFEM), which provides similar accuracy as the Multiscale Mortar Mixed FEM [3]. EVMFEM is a mass conservative and an efficient domain decomposition method. By using this method, several applications such as single, two-phase flow, bio-remediation simulation and others were considered in [3,4]. Recently, an adaptive mesh refinement strategy, which is based on Enhanced Velocity scheme, has been proposed in the numerical simulations of flow and transport through heterogeneous porous media [1,2,5,6]. Such a novel approach demonstrates the efficiency and accuracy of simulation in the heterogeneous porous media by allowing to capture important features of flow and transport problems.

A little attention has been given to discrete time setting analysis. Theoretical convergence analysis of EVMFEM has been shown in [4] for slightly compressible single phase flow for general continuous in time approximations. However, we could

* Corresponding author at: Center for Subsurface Modeling, Oden Institute for Computational Engineering and Sciences, University of Texas at Austin, 201 East 24th St, Stop C0200, POB 4.102, Austin, TX, USA.
E-mail address: yerlan.amanbek@nu.edu.kz (Y. Amanbek).

https://doi.org/10.1016/j.cam.2019.05.009
0377-0427/

not find the numerical error tests that compare with analytical solution. A few authors have begun to implement time domain decomposition method to be flexible on selection of time step size [7–9]. The key idea is to extend the EVMFEM in space to time discretization by constructing a monolithic system without subdomain iteration.

In this paper, we are concerned with the solution of time dependent problem that is discretized by the backward Euler method or the Crank–Nicolson method combined with EVMFEM, which uses the lowest order Raviart–Thomas spaces on non-matching multiple subdomains. In particularly, we focus on deriving a *priori* error estimates for the transient subsurface problems in discrete-time setting. This gives asymptotive behavior of the numerical error for a given mesh size, time step size and others. This analysis allows us to conclude about the convergence and the guarantee of stability of the numerical method. The reader is referred to [10,11] for more different time and space discretization in the transient problems. We also provide numerical tests of the error estimate.

This paper is organized as follows. In the next section, we describe the slightly compressible flow model formulation as well as give a strong and weak formulation using Enhanced Velocity space. Section 3 is devoted to the error analysis with preliminary projections, definitions and discrete formulation. This analysis carried out for backward Euler scheme and Crank–Nicolson schemes simultaneously in time discretization settings. Numerical results are presented in Section 4; Section 5 concludes the paper.

2. Model formulation

We describe in this section the slightly compressible flow formulate with initial and boundary conditions. Next, the transient problem is presented in the strong and weak formulations.

2.1. Slightly compressible flow formulation

Our focus is a single phase and slightly compressible fluid in heterogeneous porous media. The classical mass conservation equation is defined by

$$\frac{\partial}{\partial t}(\phi\rho) + \nabla\cdot(\rho\mathbf{u}) = q \qquad \text{in} \quad \Omega\times J \tag{1}$$

where $\Omega \in \mathbb{R}^d (d = 1, 2 \text{ or } 3)$, $J = (0, T]$, d is the number of spatial dimensions, q is the source/sink term, ϕ is the porosity, ρ is the phase density, and $\mathbf{u}$ is the phase velocity. We remark that a Peaceman correction is used for modeling source/sink terms [12].

In slightly compressible fluid, the phase density is given by $\rho = \rho_{ref} e^{C_f(p-p_{ref})}$, where, C_f is the fluid compressibility, and ρ_{ref} is the reference density at reference pressure p_{ref}. Using Taylor series expansion we obtain $\rho \approx \rho_{ref}(1 + C_f(p - p_{ref}))$. Then it follows that

$$\phi\frac{\partial\rho}{\partial t} = \phi\frac{\partial\rho}{\partial p}\frac{\partial p}{\partial t} = \phi C_1\frac{\partial p}{\partial t} \tag{2}$$

for invariant-in-time ϕ and for $C_1 = C_f\rho_{ref}$. The phase velocity $\mathbf{u}$ is defined by Darcy's law as,

$$\mathbf{u} = -\frac{\mathbf{K}}{\mu}(\nabla p - \rho\mathbf{g}), \tag{3}$$

where, μ is the viscosity, $\mathbf{K}$ is the permeability (absolute permeability) tensor, ρ is the density of the fluid and $\mathbf{g}$ is the gravity vector. Although more general global boundary conditions can also be treated, we restrict ourselves to the following,

$$p = g \quad \text{on} \quad \partial\Omega\times J\ . \tag{4}$$

Additionally, the initial condition is given by,

$$p(x, 0) = p^0(x). \tag{5}$$

From now on our analysis focus on a transient (parabolic) problems which might be involved to various applications problems.

2.2. Transient problem with EVMFEM

We start with the strong formulation of the transient (slightly compressible) flow problems governing single phase flow model for pressure p and the velocity $\mathbf{u}$, which is also case of slightly compressible single phase flow model:

$$\mathbf{u} = -\mathbf{K}\nabla p \qquad \text{in} \quad \Omega\times J, \tag{6}$$

$$\frac{\partial p}{\partial t} + \nabla\cdot\mathbf{u} = f \qquad \text{in} \quad \Omega\times J, \tag{7}$$

$$p = g \qquad \text{on} \quad \partial\Omega\times J \tag{8}$$

$$p = p_0 \qquad at \quad t = 0 \tag{9}$$

where $\Omega \subset \mathbb{R}^d (d = 2 \text{ or } 3)$ is multiblock domain, $J = [0, T]$ and $\mathbf{K}$ is a symmetric, uniformly positive definite tensor representing the permeability divided by the viscosity with $L^\infty(\Omega)$ components, for some $0 < k_{min} < k_{max} < \infty$

$$k_{min}\xi^T\xi \le \xi^T\mathbf{K}(x)\xi \le k_{max}\xi^T\xi \qquad \forall x \in \Omega \quad \forall \xi \in \mathbb{R}^d, d = 1, 2, 3. \tag{10}$$

Let Ω be a polygonal domain with boundary $\partial\Omega$ divided into a series of small subdomains. To formulate in mixed variational form, Sobolev spaces are exploited and the following space is defined for flux in $\mathbb{R}^d$ as usual to be $\mathbf{V} = H(\text{div}; \Omega) = \{\mathbf{v} \in \left(L^2(\Omega)\right)^d : \nabla \cdot \mathbf{v} \in L^2(\Omega)\}$ and for the pressure the space is $W = L^2(\Omega)$. In analysis we have made of use of standard notations, for more details see [3,6]. For subdomain $\zeta \subset \mathbb{R}^d$, we denote the $L^2(\zeta)$ inner product (or duality pairing) and norm by $(\cdot,\cdot)_S$ and $\|\cdot\|_\zeta$, respectively, for scalar and vector valued functions. Let $W^{m,p}$ be the standard Sobolev space of m-differentiable functions in $L^p(\zeta)$. Let $\|\cdot\|_{m,\zeta}$ be norm of $H^m(\zeta) = W^{m,2}(\zeta)$ or $H^m(\zeta)$, where ζ and m are omitted in case of $\zeta = \Omega$ and $m = 0$ respectively, in other cases they are specified. We denote $(\cdot,\cdot)$ for the $L^2(\zeta)$ or $\left(L^2(\zeta)\right)^d$ inner product, and $\langle\cdot,\cdot\rangle_{\partial\zeta}$ for duality pairing on boundaries and interfaces, where the pairing may be between two functions in L^2 or between elements of $H^{1/2}$ and $H^{-1/2}$, in either order.

The Dirichlet boundary condition is considered for convenience. A weak solution of parabolic Eqs. (6)–(9) is a pair $\{\mathbf{u}, p\} : J \to \mathbf{V} \times W$,

$$\left(K^{-1}\mathbf{u}, \mathbf{v}\right) = (p, \nabla \cdot \mathbf{v}) - \langle g, \mathbf{v} \cdot \nu\rangle_{\partial\Omega} \qquad \forall \mathbf{v} \in \mathbf{V} \tag{11}$$

$$\left(\frac{\partial p}{\partial t}, w\right) + (\nabla \cdot \mathbf{u}, w) = (f, w) \qquad \forall w \in W \tag{12}$$

In addition, there is an initial condition

$$(p, w)\Big|_{t=0} = (p_0, w) \qquad \forall w \in W \tag{13}$$

Discrete formulation

We consider $\Omega = \left(\bigcup_{i=1}^{N_d} \bar{\Omega}_i\right)^o$, $\Gamma_{i,j} = \partial\Omega_i \bigcap \partial\Omega_j$, $\Gamma = \left(\bigcup_{i,j=1}^{N_d} \bar{\Gamma}_{i,j}\right)^o$, $\Gamma_i = \Omega_i \bigcap \Gamma = \partial\Omega_j \setminus \partial\Omega$. This implies that the domain is divided into N_d subdomains, the interface between ith and jth subdomains($i \neq j$), the interior subdomain interface for ith subdomain and union of all such interfaces, respectively.

Let $\mathcal{T}_{h,i}$ be a conforming, quasi-uniform and rectangular partition of Ω_i, $1 \le i \le N_d$, with maximal element diameter h_i. We then set $\mathcal{T}_h = \cup_{i=1}^n \mathcal{T}_{h,i}$ and denote h the maximal element diameter in $\mathcal{T}_h$; note that $\mathcal{T}_h$ can be nonmatching as neighboring meshes $\mathcal{T}_{h,i}$ and $\mathcal{T}_{h,j}$ need not match on $\Gamma_{i,j}$. We assume that all mesh families are shape-regular, which ensures that the mesh elements are not highly elongated nor degenerate nearly to triangles.

We will consider in our work the Raviart–Thomas spaces of lowest order on rectangles for $d = 2$ and bricks for $d = 3$. The RT_0 spaces are defined for any element $T \in \mathcal{T}_h$ by the following spaces: $\mathbf{V}_h(T) = \{\mathbf{v} = (v_1, v_2)$ or $\mathbf{v} = (v_1, v_2, v_3) : v_l = \alpha_l + \beta_l x_l : \alpha_l, \beta_l \in \mathbb{R}; l = 1, ..d\}$ and $W_h(T) = \{w = \text{constant}\}$ In fact, a vector function in $\mathbf{V}_h$ can be determined uniquely by its normal components $\mathbf{v} \cdot \nu$ at midpoints of edges (in 2D) or face (in 3D) of T. The degrees of freedom of $\mathbf{v} \in \mathbf{V}_h(T)$ were created by these normal components. The degree of freedom for a pressure function $p \in W_h(T)$ is at center of T and piecewise constant inside of T. The pressure finite element approximation space on Ω is taken to be as

$$W_h(\Omega) = \{w \in L^2(\Omega) : w\Big|_E \in W_h(T), \forall T \in \mathcal{T}_h\}$$

The next step is to construct a velocity finite element approximation space on Ω. Let us formulate RT_0 space on each subdomain Ω_i for partition $\mathcal{T}_h$

$$\mathbf{V}_{h,i} = \{\mathbf{v} \in H(\text{div}; \Omega_i) : \mathbf{v}\Big|_T \in \mathbf{V}_h(T), \forall T \in \mathcal{T}_{h,i}\} \qquad i \in \{1, \ldots, n\}$$

and then

$$\mathbf{V}_h = \bigoplus_{i=1}^n \mathbf{V}_{h,i}.$$

Although the normal components of vectors in $\mathbf{V}_h$ are continuous between elements within each subdomains, the reader may see $\mathbf{V}_h$ is *not* a subspace of $H(\text{div}; \Omega)$, because the normal components of the velocity vector may not match on subdomain interface Γ. To solve this issue, many researchers have proposed various methods such as Multiscale Mortar Mixed FEM [13], Enhanced Velocity Mixed FEM [3], etc. In Mortar Multiscale Mixed FEM , the mortar finite element space on coarse grid was introduced to connect subdomains together using Lagrange multipliers to enforce weak continuity for flux across subdomains. On the other hand, the Enhanced Velocity Mixed FEM modifies the degree of freedom on Γ to finer grids, which impose the strong flux continuity between subdomains. Let us define $\mathcal{T}_{h,i,j}$ as the intersection of the traces of $\mathcal{T}_{h,i}$ and $\mathcal{T}_{h,j}$, and let $\mathcal{T}_h^\Gamma = \bigcup_{1\le i\le j\le N_d} \mathcal{T}_{h,i,j}$. We require that $\mathcal{T}_{h,i}$ and $\mathcal{T}_{h,j}$ need to align with the coordinate axes. Fluxes are constructed to match on each element $e \in \mathcal{T}_h^\Gamma$. We consider any element $T \in \mathcal{T}_{h,i}$ that shares at least one edge

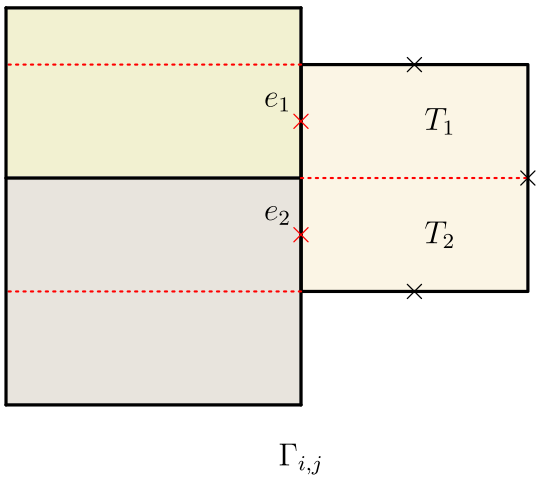

Fig. 2.1. Degrees of freedom for the Enhanced Velocity space.

with the interface Γ, i.e., $T \cap \Gamma_{i,j} \neq \emptyset$, where $1 \leq i, j \leq N_d$ and $i \neq j$. Then newly defined interface grid introduces a partition of the edge of T. This partition may be extended into the element T as shown in Fig. 2.1. This new partitioning helps to construct fine-scale fluxes that is in $H(\text{div}, \Omega)$. So we represent a basis function $\mathbf{v}_{T_k}$ in the $\mathbf{V}_h(T_k)$ space (RT_0) for given T_k with the following way:

$$\mathbf{v}_{T_k} \cdot \nu = \begin{cases} 1, & \text{on } e_k \\ 0, & \text{other edges} \end{cases}$$

i.e. a normal component $\mathbf{v}_{T_k} \cdot \nu$ equal to one on e_k and zero on all other edges(faces) of T_k. Let $\mathbf{V}_h^{\Gamma}$ be span of all such basis functions defined on all sub-elements induced the interface discretization $\mathcal{T}_{h,i,j}$. Thus, the enhanced velocity space $\mathbf{V}_h^*$ is taken to be as

$$\mathbf{V}_h^* = \bigoplus_{i=1}^{n} \mathbf{V}_{h,i}^0 \bigoplus \mathbf{V}_h^{\Gamma} \cap H(\text{div}; \Omega).$$

where $\mathbf{V}_{h,i}^0 = \{\mathbf{v} \in \mathbf{V}_{h,i} : \mathbf{v} \cdot \nu = 0 \text{ on } \Gamma_i\}$ is the subspace of $\mathbf{V}_{h,i}$. The finer grid flux allows to velocity approximation on the interface and then form the $H(\text{div}, \Omega)$ conforming velocity space. Some difficulties arise, however, in analysis of method and implementation of robust linear solver for such modification of RT_0 velocity space at all elements, which are adjacent to the interface Γ.

We formulate the variational problem in semi-discrete space as: Find $\{\mathbf{u}_h, p_h\} : J \to \mathbf{V}_h^* \times W_h$ such that

$$\left(\mathbf{K}^{-1}\mathbf{u}_h, \mathbf{v}\right) = (p_h, \nabla \cdot \mathbf{v}) - \langle g, \mathbf{v} \cdot \nu \rangle_{\partial\Omega} \qquad \forall \mathbf{v} \in \mathbf{V}_h^* \tag{14}$$

$$\left(\frac{\partial p_h}{\partial t}, w\right) + (\nabla \cdot \mathbf{u}_h, w) = (f, w) \qquad \forall w \in W_h \tag{15}$$

In addition, there is an initial condition

$$(p_h, w)\Big|_{t=0} = (p_0, w) \qquad \forall w \in W_h \tag{16}$$

Subtracting Eqs. (11)–(12) from Eqs. (14)–(15) yields

$$\left(\mathbf{K}^{-1}(\mathbf{u} - \mathbf{u}_h), \mathbf{v}\right) - (p - p_h, \nabla \cdot \mathbf{v}) = 0 \qquad \forall \mathbf{v} \in \mathbf{V}_h^* \tag{17}$$

$$\left(\frac{\partial}{\partial t}(p - p_h), w\right) + (\nabla \cdot (\mathbf{u} - \mathbf{u}_h), w) = 0 \qquad \forall w \in W_h \tag{18}$$

3. Error estimates

In this section, we start with preliminaries including projections operators and some notations. Using them we present discrete formulations for analysis. Next, we derive auxiliary error estimates and a *priori* error estimate theorems.

3.1. Projections

We shall write a projection and define auxiliary error of pressure and velocity as follows:

$$E_p^I = p - \hat{p}, \qquad E_p^A = \hat{p} - p_h, \tag{19}$$

$$E_{\mathbf{u}}^I = \mathbf{u} - \Pi^*\mathbf{u}, \qquad E_{\mathbf{u}}^A = \Pi^*\mathbf{u} - \mathbf{u}_h. \tag{20}$$

Note that $\mathbf{u} - \mathbf{u}_h = E_{\mathbf{u}}^I + E_{\mathbf{u}}^A$, $p - p_h = E_p^I + E_p^A$. We used $\hat{p}$ the L^2-projection of p that is defined as

$$\left(p - \hat{p}, w\right) = \left(E_p^I, w\right) = 0 \qquad \forall w \in W_h. \tag{21}$$

We know from original work [3] that the projection operator Π^* was introduced and was utilized for a *priori* error analysis of elliptic problems. For convenience of the reader, we repeat the relevant and brief definition. Thus, we denote by Π^* the projection operator that maps $(H^1(\Omega))^d$ onto $\mathbf{V}_h^*$ that defined locally for any element $T \in \mathcal{T}_h$ and any $\mathbf{q} \in (H^1(T))^d$ such that

$$\langle \Pi^*\mathbf{q} \cdot \nu, 1\rangle_e = \langle \mathbf{q} \cdot \nu, 1\rangle_e \tag{22}$$

where e is either any edge in 2D (or face in 3D) of T not lying on Γ or an edge in 2D (or face in 3D) of a sub-element, T_k. Such projection is developed prior to conducting error analysis for a *priori* estimate. As can be seen in Fig. 2.1, T_k has a common edge with the interface grid $\mathcal{T}^\Gamma$. According to divergence theorem, we have

$$\left(\nabla \cdot (\Pi^*\mathbf{q} - \mathbf{q}), w\right) = 0 \qquad \forall w \in W_h \tag{23}$$

For $\mathbf{u} \in H^1(\Omega)$

$$\left(\nabla \cdot \left(\Pi^*\mathbf{u} - \mathbf{u}\right), w\right) = \left(\nabla \cdot E_{\mathbf{u}}^I, w\right) = 0 \qquad \forall w \in W_h \tag{24}$$

Lemma.

$$\left(\frac{\partial}{\partial t}E_p^I, w\right) = 0 \qquad \forall w \in W_h \tag{25}$$

Proof. $0 = \frac{d}{dt}\left(E_p^I, w\right) = \left(\frac{\partial}{\partial t}E_p^I, w\right) + \cancelto{0}{\left(E_p^I, w_t\right)}$, by (21), since $w_t \in W_h$. □

Useful inequalities of projections , see [3]:

$$\left\|E_p^I\right\| \le C\|p\|_r h^r \qquad 0 \le r \le 1, \tag{26}$$

$$\left\|E_{\mathbf{u}}^I\right\| \le C\|\mathbf{u}\|_1 h. \tag{27}$$

Recall Young's Inequality: for $a, b \ge 0$

$$ab \le \frac{1}{2\varepsilon}a^2 + \frac{\varepsilon}{2}b^2 \tag{28}$$

The Inverse Inequality can be given as

$$\|\nabla \cdot \mathbf{u}_h\| \le Ch^{-1}\|\mathbf{u}_h\| \tag{29}$$

In this inequality, we have been working under the assumption that $\mathcal{T}_{h,i}$ quasi-uniform rectangular partition of Ω_i.

3.2. Definitions

In this section, we make analysis of discrete in time error estimates. Firstly, some definitions are made: for $\Delta t = \frac{T}{N}$, N is a positive integer, $t_n = n\Delta t$ and for given $\theta \in [0, 1]$,

$$f^n = f(x, t_n), \qquad 0 \le n \le N, \tag{30}$$

$$f^{n,\theta} = \frac{1}{2}(1+\theta)f^{n+1} + \frac{1}{2}(1-\theta)f^n, \qquad 0 \le n \le N-1. \tag{31}$$

Let us make also the following definitions:

$$\|f\|_{l^\infty(L^2)} = \max_{0\le n\le N}\left\|f^n\right\|_{L^2}$$

$$\|f\|_{l^2(L^p)} = \left(\sum_{n=0}^{N-1}\left\|f^{n,\theta}\right\|_{L^p}^2 \Delta t\right)^{\frac{1}{2}}.$$

We note that the difference can be expressed $t^{n,\theta} - t^n = \frac{1}{2}(1+\theta)\Delta t$. Next, using the Taylor series expansion about $t = t^{n,\theta}$, for any sufficiently smooth function $f(t)$, we obtain:

$$f^{n+1} = f\Big|_{t=t^{n,\theta}} + \frac{1}{2}(1-\theta)\Delta t \frac{\partial f}{\partial t}\Big|_{t=t^{n,\theta}} + \frac{1}{8}(1-\theta)^2(\Delta t)^2 \frac{\partial^2 f}{\partial t^2}\Big|_{t=t^{n,\theta}} + O(\Delta t^3)$$

$$f^{n} = f\Big|_{t=t^{n,\theta}} - \frac{1}{2}(1+\theta)\Delta t \frac{\partial f}{\partial t}\Big|_{t=t^{n,\theta}} + \frac{1}{8}(1+\theta)^2(\Delta t)^2 \frac{\partial^2 f}{\partial t^2}\Big|_{t=t^{n,\theta}} + O(\Delta t^3)$$

After multiplying the first equation by $\frac{1}{2}(1+\theta)$ and the second equation by $\frac{1}{2}(1-\theta)$ and then summing them, we obtain

$$f^{n,\theta} = f\Big|_{t=t^{n,\theta}} + \frac{1}{8}(\Delta t)^2(1+\theta)(1-\theta)\frac{\partial^2 f}{\partial t^2}\Big|_{t=t^{n,\theta}} + O(\Delta t^3)$$

Note that if $\theta = 1$ then $f^{n,\theta} = f\Big|_{t=t^{n,\theta}} + O(\Delta t^3)$. In addition, we can get second order approximation of Δt, details in [14] : $p(\mathbf{x}, t^{n,\theta}) \approx p^{n,\theta}$ and $\mathbf{u}(\mathbf{x}, t^{n,\theta}) \approx \mathbf{u}^{n,\theta}$. According to Taylor series expansion [14], we obtain

$$\frac{p^{n+1} - p^n}{\Delta t} = p_t(x, t^{n,\theta}) + \rho^{p,n,\theta}, \qquad \forall x \in \Omega, \tag{32}$$

where $\rho^{p,n,\theta}$ depends on time-derivatives of p and Δt and one of its property as follows

$$\left\|\rho^{p,n,\theta}\right\| \leq \begin{cases} C_1 \Delta t \|p_{tt}\|_{L^\infty((t^n,t^{n+1}),H^1)}, & \text{if} \quad \theta = 1, \\ C_2 \Delta t^2 \|p_{ttt}\|_{L^\infty((t^n,t^{n+1}),H^1)}, & \text{if} \quad \theta = 0, \end{cases} \tag{33}$$

so $\left\|\rho^{p,n,\theta}\right\| = \mathcal{O}(\Delta t\theta + \Delta t^2\left((1-\theta)^3 + (1+\theta)^3\right))$.

3.3. Discrete formulation

We formulate variational form in semi-discrete space as: Find $\{\mathbf{u}_h, p_h\} : J \to \mathbf{V}_h^* \times W_h$ such that

$$\left(\frac{\partial p_h}{\partial t}, w\right) + (\nabla \cdot \mathbf{u}_h, w) = l_1(w) \qquad \forall w \in W_h \tag{34}$$

$$\left(\mathbf{K}^{-1}\mathbf{u}_h, \mathbf{v}\right) - (p_h, \nabla \cdot \mathbf{v}) = l_2(\mathbf{v}) \qquad \forall \mathbf{v} \in \mathbf{V}_h^* \tag{35}$$

In addition, there is an initial condition

$$(p_h, w)\Big|_{t=0} = (p_0, w) \qquad \forall w \in W_h \tag{36}$$

where l_1 and l_2 are bounded linear functionals, i.e.

$$l_1(w) = (f, w),$$
$$l_2(\mathbf{v}) = -\langle g, \mathbf{v} \cdot \nu\rangle_{\partial\Omega}.$$

We shall write $l_1^{n,\theta} = (f^{n,\theta}, w)$ and $l_2^{n,\theta} = -\langle g^{n,\theta}, \mathbf{v} \cdot \nu\rangle_{\partial\Omega}$.

With these definitions, Eqs. (34)–(35) become as: Find $\{\mathbf{u}_h^{n,\theta}, p_h^{n,\theta}\} \in \mathbf{V}_h^* \times W_h$, $n = 1, 2, \ldots, N-1$, such that

$$\left(\frac{p_h^{n+1} - p_h^n}{\Delta t}, w\right) + \left(\nabla \cdot \mathbf{u}_h^{n,\theta}, w\right) = l_1^{n,\theta}(w) + \left(\rho^{p,n,\theta}, w\right) \qquad \forall w \in W_h \tag{37}$$

$$\left(\mathbf{K}^{-1}\mathbf{u}_h^{n,\theta}, \mathbf{v}\right) - \left(p_h^{n,\theta}, \nabla \cdot \mathbf{v}\right) = l_2^{n,\theta}(\mathbf{v}) \qquad \forall \mathbf{v} \in \mathbf{V}_h^* \tag{38}$$

Note that if $\theta = 1$ then the time discretization is the backward Euler(Implicit) method, and if $\theta = 0$ then the Crank–Nicolson scheme.

We consider true solution $\mathbf{u} \in L^2(J, \mathbf{V})$ and $p_h \in H^1(J, W)$ of Eqs. (11) and (12) at time $t = t^{n,\theta}$ in the continuous in time with spatially discrete scheme. We used Eq. (32) and additional remark related to the Taylor series expansion in order to obtain the following equations with at least order of $\mathcal{O}(\Delta t)$:

$$\left(\frac{p^{n+1} - p^n}{\Delta t}, w\right) + \left(\nabla \cdot \mathbf{u}^{n,\theta}, w\right) = \left(f(t^{n,\theta}, \cdot), w\right) + \left(\rho^{p,n,\theta}, w\right) \qquad \forall w \in W \tag{39}$$

$$\left(K^{-1}\mathbf{u}^{n,\theta}, \mathbf{v}\right) - \left(p^{n,\theta}, \nabla \cdot \mathbf{v}\right) = -\langle g^{n,\theta}, \mathbf{v} \cdot \nu\rangle_{\partial\Omega} \qquad \forall \mathbf{v} \in \mathbf{V} \tag{40}$$

We approximate the vector integrals type $(\mathbf{v}, \mathbf{q})_{T,M}$ by trapezoidal-midpoint quadrature rules and $\left(\mathbf{K}^{-1}\mathbf{q}, \mathbf{v}\right)_T$ by trapezoidal quadrature rules respectively. In [15], the equivalence between finite volume methods and the mixed

finite element method was established for special quadrature rule for $\mathbf{K}$ diagonal tensor and using the lowest-order Raviart–Thomas spaces on rectangles. We emphasize that the EVMFEM with special quadrature and velocity elimination in the discrete system can be reduced to well-known a cell-centered finite difference method.

For each time step we use the Newton method to solve the system, in case of the slightly compressible flow: the fluid compressibility C_f term brings us to a nonlinear system. That is why consideration of it would be beneficial for nonlinear problems in the future.

3.4. Analysis

We first derive the bounds of auxiliary error terms.

Theorem 1 (*Auxiliary Error Estimate*). *For the velocity $\mathbf{u_h}$ and pressure p_h of the mixed method spaces $\mathbf{V}_h^* \times W_h$ satisfying equations (37)–(38), assume Δt is sufficiently small and positive, $\mathbf{K}$ is uniformly positive definite and sufficient regularity of true solution in Eqs. (6)–(9). Then, there exists a constant C such that*

$$\left\|E_{\mathbf{u}}^{A}\right\|_{l^2(L^2)}^2 + \left\|E_p^A\right\|_{l^\infty(L^2)}^2 \le C\left(h^2 + h + \Delta t^{2r}\right) \tag{41}$$

where $C = C(T, \mathbf{K}, \mathbf{u}, p)$ and

$$r = \begin{cases} 1, & \text{if} \quad \theta = 1 \\ 2, & \text{if} \quad \theta = 0 \end{cases}$$

Proof. Subtracting Eqs. (39)–(40) from Eqs. (37)–(38) respectively yields

$$\left(\frac{p^{n+1} - p_h^{n+1} - \left(p^n - p_h^n\right)}{\Delta t}, w\right) + \left(\nabla \cdot \left(\mathbf{u}^{n,\theta} - \mathbf{u}_h^{n,\theta}\right), w\right) = \left(\rho^{p,n,\theta}, w\right) \quad \forall w \in W_h \tag{42}$$

$$\left(K^{-1}\left(\mathbf{u}^{n,\theta} - \mathbf{u}_h^{n,\theta}\right), \mathbf{v}\right) - \left(p^{n,\theta} - p_h^{n,\theta}, \nabla \cdot \mathbf{v}\right) = 0 \quad \forall \mathbf{v} \in \mathbf{V}_h^*. \tag{43}$$

Take $\mathbf{v} = \Pi^* \mathbf{u}^{n,\theta} - \mathbf{u}_h^{n,\theta} = E_{\mathbf{u}}^{A\,n,\theta}$ and $w = E_p^{A\,n,\theta}$ in (43) and (42) respectively.

$$\left(\frac{\left(E_p^{I\,n+1} + E_p^{A\,n+1}\right) - \left(E_p^{I\,n} + E_p^{A\,n}\right)}{\Delta t}, E_p^{A\,n,\theta}\right)$$
$$+ \left(\nabla \cdot \left(E_{\mathbf{u}}^{I\,n,\theta} + E_{\mathbf{u}}^{A\,n,\theta}\right), E_p^{A\,n,\theta}\right) = \left(\rho^{p,n,\theta}, E_p^{A\,n,\theta}\right)$$
$$\left(\mathbf{K}^{-1}\left(E_{\mathbf{u}}^{I\,n,\theta} + E_{\mathbf{u}}^{A\,n,\theta}\right), E_{\mathbf{u}}^{A\,n,\theta}\right) - \left(E_p^{I\,n,\theta} + E_p^{A\,n,\theta}, \nabla \cdot E_{\mathbf{u}}^{A\,n,\theta}\right) = 0$$

After adding them, we can rewrite as

$$\underbrace{\left(\frac{\left(E_p^{I\,n+1} + E_p^{A\,n+1}\right) - \left(E_p^{I\,n} + E_p^{A\,n}\right)}{\Delta t}, E_p^{A\,n,\theta}\right)}_{\mathbb{F}_1} + \underbrace{\left(\nabla \cdot \left(E_{\mathbf{u}}^{I\,n,\theta} + E_{\mathbf{u}}^{A\,n,\theta}\right), E_p^{A\,n,\theta}\right)}_{\mathbb{F}_2} +$$
$$+ \underbrace{\left(\mathbf{K}^{-1}\left(E_{\mathbf{u}}^{I\,n,\theta} + E_{\mathbf{u}}^{A\,n,\theta}\right), E_{\mathbf{u}}^{A\,n,\theta}\right)}_{\mathbb{F}_3} - \underbrace{\left(E_p^{I\,n,\theta} + E_p^{A\,n,\theta}, \nabla \cdot E_{\mathbf{u}}^{A\,n,\theta}\right)}_{\mathbb{F}_4} = \left(\rho^{p,n,\theta}, E_p^{A\,n,\theta}\right)$$

$$\mathbb{F}_1 = \left(\frac{E_p^{I\,n+1} - E_p^{I\,n}}{\Delta t}, E_p^{A\,n,\theta}\right) + \left(\frac{E_p^{A\,n+1} - E_p^{A\,n}}{\Delta t}, E_p^{A\,n,\theta}\right)$$
$$= \left(\frac{E_p^{A\,n+1} - E_p^{A\,n}}{\Delta t}, E_p^{A\,n,\theta}\right)$$

In here we have made use of approximation

$$\frac{E_p^{I\,n+1} - E_p^{I\,n}}{\Delta t} \approx \left(E_p^{I\,n,\theta}\right)_t + O(\Delta t\theta + \Delta t^2((1-\theta)^3 + (1+\theta)^3))$$

and the property (25).

$$\mathbb{F}_2 - \mathbb{F}_4 = \left(\nabla \cdot E_{\mathbf{u}}^{I\,n,\theta}, E_p^{A\,n,\theta}\right) + \left(\nabla \cdot E_{\mathbf{u}}^{A\,n,\theta}, E_p^{A\,n,\theta}\right)$$
$$- \left(E_p^{I\,n,\theta}, \nabla \cdot E_{\mathbf{u}}^{A\,n,\theta}\right) - \left(E_p^{A\,n,\theta}, \nabla \cdot E_{\mathbf{u}}^{A\,n,\theta}\right)$$

$$= \underbrace{\left(\nabla \cdot E_{\mathbf{u}}^{I\,n,\theta}, E_p^{A\,n,\theta}\right)}_{0,\ \text{by (24)}} - \left(E_p^{I\,n,\theta}, \nabla \cdot E_{\mathbf{u}}^{A\,n,\theta}\right)$$
$$= -\left(E_p^{I\,n,\theta}, \nabla \cdot E_{\mathbf{u}}^{A\,n,\theta}\right)$$

After replacing terms in $\mathbb{F}_1$, $\mathbb{F}_2$, $\mathbb{F}_4$ and extending terms in $\mathbb{F}_3$, we thus obtain the equation

$$\left(\frac{E_p^{A\,n+1} - E_p^{A\,n}}{\Delta t}, E_p^{A\,n,\theta}\right) + \left(\mathbf{K}^{-1} E_{\mathbf{u}}^{A\,n,\theta}, E_{\mathbf{u}}^{A\,n,\theta}\right) \tag{44}$$
$$= -\left(\mathbf{K}^{-1} E_{\mathbf{u}}^{I\,n,\theta}, E_{\mathbf{u}}^{A\,n,\theta}\right) + \left(E_p^{I\,n,\theta}, \nabla \cdot E_{\mathbf{u}}^{A\,n,\theta}\right) + \left(\rho^{p,n,\theta}, E_p^{A\,n,\theta}\right)$$

We need a useful inequality for the next step, therefore, we consider the following term,

$$\left(\frac{E_p^{A\,n+1} - E_p^{A\,n}}{\Delta t}, E_p^{A\,n,\theta}\right) = \left(\frac{E_p^{A\,n+1} - E_p^{A\,n}}{\Delta t}, \frac{1+\theta}{2} E_p^{A\,n+1} + \frac{1-\theta}{2} E_p^{A\,n}\right)$$
$$= \frac{1+\theta}{2\Delta t}\left(E_p^{A\,n+1}, E_p^{A\,n+1}\right) - \frac{1+\theta}{2\Delta t}\left(E_p^{A\,n}, E_p^{A\,n+1}\right)$$
$$+ \frac{1-\theta}{2\Delta t}\left(E_p^{A\,n+1}, E_p^{A\,n}\right) - \frac{1-\theta}{2\Delta t}\left(E_p^{A\,n}, E_p^{A\,n}\right)$$
$$= \frac{1+\theta}{2\Delta t}\left\|E_p^{A\,n+1}\right\|^2 - \frac{2\theta}{2\Delta t}\left(E_p^{A\,n}, E_p^{A\,n+1}\right) - \frac{1-\theta}{2\Delta t}\left\|E_p^{A\,n}\right\|^2$$
$$= \frac{1}{2\Delta t}\left(\left\|E_p^{A\,n+1}\right\|^2 - \left\|E_p^{A\,n}\right\|^2\right) + \underbrace{\frac{\theta}{2\Delta t}\left(\left\|E_p^{A\,n+1}\right\| - \left\|E_p^{A\,n}\right\|\right)^2}_{\geq 0} \geq$$
$$\geq \frac{1}{2\Delta t}\left(\left\|E_p^{A\,n+1}\right\|^2 - \left\|E_p^{A\,n}\right\|^2\right)$$

It follows immediately the useful inequality

$$\left(\frac{E_p^{A\,n+1} - E_p^{A\,n}}{\Delta t}, E_p^{A\,n,\theta}\right) \geq \frac{1}{2\Delta t}\left(\left\|E_p^{A\,n+1}\right\|^2 - \left\|E_p^{A\,n}\right\|^2\right) \tag{45}$$

By using (45), multiply by $2\Delta t$ and sum from 0 to $N-1$ in Eq. (44).

$$\sum_{n=0}^{N-1}\left(\left\|E_p^{A\,n+1}\right\|^2 - \left\|E_p^{A\,n}\right\|^2\right) + 2\sum_{n=0}^{N-1}\left(\mathbf{K}^{-1} E_{\mathbf{u}}^{A\,n,\theta}, E_{\mathbf{u}}^{A\,n,\theta}\right)\Delta t \leq$$
$$\leq -2\sum_{n=0}^{N-1}\left(\mathbf{K}^{-1} E_{\mathbf{u}}^{I\,n,\theta}, E_{\mathbf{u}}^{A\,n,\theta}\right)\Delta t + 2\sum_{n=0}^{N-1}\left(E_p^{I\,n,\theta}, \nabla \cdot E_{\mathbf{u}}^{A\,n,\theta}\right)\Delta t + 2\sum_{n=0}^{N-1}\left(\rho^{p,n,\theta}, E_p^{A\,n,\theta}\right)\Delta t$$
$$\underbrace{\left(\left\|E_p^{A\,N}\right\|^2 - \left\|E_p^{A\,0}\right\|^2\right)}_{0,\ \text{by (36)}} + \sum_{n=0}^{N-1}\left(\mathbf{K}^{-1} E_{\mathbf{u}}^{A\,n,\theta}, E_{\mathbf{u}}^{A\,n,\theta}\right)\Delta t$$
$$\leq \underbrace{-2\sum_{n=0}^{N-1}\left(\mathbf{K}^{-1} E_{\mathbf{u}}^{I\,n,\theta}, E_{\mathbf{u}}^{A\,n,\theta}\right)\Delta t}_{\mathbb{T}_1} + \underbrace{2\sum_{n=0}^{N-1}\left(\rho^{p,n,\theta}, E_p^{A\,n,\theta}\right)\Delta t}_{\mathbb{T}_2} + \underbrace{2\sum_{n=0}^{N-1}\left(E_p^{I\,n,\theta}, \nabla \cdot E_{\mathbf{u}}^{A\,n,\theta}\right)\Delta t}_{\mathbb{T}_3}$$

$$\mathbb{T}_1 = -2\sum_{n=0}^{N-1}\left(\mathbf{K}^{-1} E_{\mathbf{u}}^{I\,n,\theta}, E_{\mathbf{u}}^{A\,n,\theta}\right)\Delta t$$
$$\underbrace{\leq}_{\text{Holder's ineq.}} 2\sum_{n=0}^{N-1}\left\|\mathbf{K}^{-1} E_{\mathbf{u}}^{I\,n,\theta}\right\|\left\|E_{\mathbf{u}}^{A\,n,\theta}\right\|\Delta t$$
$$\underbrace{\leq}_{\text{Young's ineq.}} \frac{1}{\varepsilon k_{min}^2}\sum_{n=0}^{N-1}\left\|E_{\mathbf{u}}^{I\,n,\theta}\right\|^2\Delta t + \varepsilon\sum_{n=0}^{N-1}\left\|E_{\mathbf{u}}^{A\,n,\theta}\right\|^2\Delta t$$

We use the Holder inequality and the Young inequality to get

$$\begin{aligned}\mathbb{T}_2 =& 2\sum_{n=0}^{N-1}\left(\rho^{p,n,\theta}, E_p^{A\,n,\theta}\right)\Delta t \le 2\sum_{n=0}^{N-1}\left\|\rho^{p,n,\theta}\right\|\left\|E_p^{A\,n,\theta}\right\|\Delta t\\ &\le \sum_{n=0}^{N-1}\left\|E_p^{A\,n}\right\|^2\Delta t + \sum_{n=0}^{N-1}\left\|\rho^{p,n,\theta}\right\|^2\Delta t.\end{aligned}$$

We define Ω^* to be the collection of the interface neighbor elements, i.e. the union of the all $T \in \mathcal{T}_h$ such that $T \cap \Gamma = \emptyset$, for details see [3]. We should note that

$$\left(E_p^I, \nabla\cdot E_u^A\right)_{\Omega} = \left(E_p^I, \nabla\cdot E_u^A\right)_{\Omega^*} + \cancelto{0}{\left(E_p^I, \nabla\cdot E_u^A\right)_{\Omega\setminus\Omega^*}} = \left(E_p^I, \nabla\cdot E_u^A\right)_{\Omega^*} \tag{46}$$

since $\nabla\cdot E_u^A\Big|_{\Omega\setminus\Omega^*} \in W_h$ and the property (21).

$$\begin{aligned}\mathbb{T}_3 &= 2\sum_{n=0}^{N-1}\left(E_p^{I\,n,\theta}, \nabla\cdot E_{\mathbf{u}}^{A\,n,\theta}\right)_{\Omega}\Delta t\\ &= 2\sum_{n=0}^{N-1}\left(E_p^{I\,n,\theta}, \nabla\cdot E_{\mathbf{u}}^{A\,n,\theta}\right)_{\Omega^*}\Delta t\\ &\le 2\sum_{n=0}^{N-1}\left\|E_p^{I\,n,\theta}\right\|_{\Omega^*}\left\|\nabla\cdot E_{\mathbf{u}}^{A\,n,\theta}\right\|_{\Omega^*}\Delta t \le\\ &\le 2C\sum_{n=0}^{N-1}\left(\frac{1+\theta}{2}\left\|p^{n+1}\right\|_{1,\Omega^*} + \frac{1-\theta}{2}\left\|p^{n}\right\|_{1,\Omega^*}\right)h\left\|E_{\mathbf{u}}^{A\,n,\theta}\right\|_{\Omega}h^{-1}\Delta t\\ &\le C\sum_{n=0}^{N-1}\left(\frac{1+\theta}{2}\left\|p^{n+1}\right\|_{1,\Omega^*} + \frac{1-\theta}{2}\left\|p^{n}\right\|_{1,\Omega^*}\right)^2\Delta t + \varepsilon\sum_{n=0}^{N-1}\left\|E_{\mathbf{u}}^{A\,n,\theta}\right\|^2\Delta t\end{aligned}$$

Remark 1. We used the following properties:

$$\begin{aligned}\left\|E_p^{I\,n,\theta}\right\|_{\Omega^*} &= \left\|\frac{1+\theta}{2}E_p^{I\,n+1} + \frac{1-\theta}{2}E_p^{I\,n}\right\|_{\Omega^*}\\ &\le \frac{1+\theta}{2}\left\|E_p^{I\,n+1}\right\|_{\Omega^*} + \frac{1-\theta}{2}\left\|E_p^{I\,n}\right\|_{\Omega^*}\\ &\le \frac{1+\theta}{2}\left\|p^{n+1}\right\|_{1,\Omega^*}h + \frac{1-\theta}{2}\left\|p^{n}\right\|_{1,\Omega^*}h\\ &\le \left(\frac{1+\theta}{2}\left\|p^{n+1}\right\|_{1,\Omega^*} + \frac{1-\theta}{2}\left\|p^{n}\right\|_{1,\Omega^*}\right)h\end{aligned}$$

and

$$\left\|\nabla\cdot E_{\mathbf{u}}^{A\,n,\theta}\right\|_{\Omega^*} \le C\left\|E_{\mathbf{u}}^{A\,n,\theta}\right\|_{\Omega^*}h^{-1} \le C\left\|E_{\mathbf{u}}^{A\,n,\theta}\right\|_{\Omega}h^{-1}$$

Next, we know that

$$\left(\mathbf{K}^{-1}E_{\mathbf{u}}^{A\,n,\theta}, E_{\mathbf{u}}^{A\,n,\theta}\right) \ge \frac{1}{k_{max}}\left\|E_{\mathbf{u}}^{A\,n,\theta}\right\|^2$$

Therefore,

$$\begin{aligned}&\frac{1}{2}\left\|E_p^{A\,N}\right\|^2 + \left[\frac{2}{k_{max}} - 2\varepsilon\right]\sum_{n=0}^{N-1}\left\|E_{\mathbf{u}}^{A\,n,\theta}\right\|^2\Delta t \le\\ &\le C\sum_{n=0}^{N-1}\left\|E_{\mathbf{u}}^{I\,n,\theta}\right\|^2\Delta t + C\sum_{n=0}^{N-1}\left\|\rho^{p,n,\theta}\right\|^2\Delta t + C\sum_{n=0}^{N-1}\left\|E_p^{A\,n}\right\|^2\Delta t +\\ &+ \frac{1}{2}\left\|E_p^{A\,N}\right\|^2\Delta t + +C\sum_{n=0}^{N-1}\left(\frac{1+\theta}{2}\left\|p^{n+1}\right\|_{1,\Omega^*} + \frac{1-\theta}{2}\left\|p^{n}\right\|_{1,\Omega^*}\right)^2\Delta t\end{aligned}$$

We can multiply by 2 and make ε small enough in order to have LHS with positive coefficients. Later take minimum and divide both sides of inequality.

$$\sum_{n=0}^{N-1} \left\| E_{\mathbf{u}}^{A\,n,\theta} \right\|^2 \Delta t + \left\| E_p^{A\,N} \right\|^2 \leq$$
$$\leq C\Delta t \left[\sum_{n=0}^{N-1} \left\| E_{\mathbf{u}}^{I\,n,\theta} \right\|^2 + \sum_{n=0}^{N-1} \left(\frac{1+\theta}{2} \left\| p^{n+1} \right\|_{1,\Omega^*} + \frac{1-\theta}{2} \left\| p^{n} \right\|_{1,\Omega^*} \right)^2 \right]$$
$$+ C \sum_{n=0}^{N-1} \left\| E_p^{A\,n} \right\|^2 \Delta t + C \sum_{n=0}^{N-1} \left\| \rho^{p,n,\theta} \right\|^2 \Delta t.$$

We thus apply the discrete Gronwall lemma, for sufficiently small Δt, to obtain:

$$\sum_{n=0}^{N-1} \left\| E_{\mathbf{u}}^{A\,n,\theta} \right\|^2 \Delta t + \left\| E_p^{A\,N} \right\|^2$$
$$\leq C\Delta t \left[\sum_{n=0}^{N-1} \left\| E_{\mathbf{u}}^{I\,n,\theta} \right\|^2 + \sum_{n=0}^{N-1} \left(\frac{1+\theta}{2} \left\| p^{n+1} \right\|_{1,\Omega^*} + \frac{1-\theta}{2} \left\| p^{n} \right\|_{1,\Omega^*} \right)^2 \right] + C \sum_{n=0}^{N-1} \left\| \rho^{p,n,\theta} \right\|^2 \Delta t$$
$$\leq C\Delta t \left[\sum_{n=0}^{N-1} \left\| E_{\mathbf{u}}^{I\,n,\theta} \right\|^2 + h \sum_{n=0}^{N-1} \left(\frac{1+\theta}{2} \left\| p^{n+1} \right\|_{1,\infty,\Omega^*} + \frac{1-\theta}{2} \left\| p^{n} \right\|_{1,\infty,\Omega^*} \right)^2 \right] + C \sum_{n=0}^{N-1} \left\| \rho^{p,n,\theta} \right\|^2 \Delta t$$
$$\leq Ch^2 \sum_{n=0}^{N-1} \left(\frac{1+\theta}{2} \left\| u^{n+1} \right\|_1 + \frac{1-\theta}{2} \left\| u^{n} \right\|_1 \right)^2 \Delta t +$$
$$+ Ch \sum_{n=0}^{N-1} \left(\frac{1+\theta}{2} \left\| p^{n+1} \right\|_{1,\infty,\Omega^*} + \frac{1-\theta}{2} \left\| p^{n} \right\|_{1,\infty,\Omega^*} \right)^2 \Delta t + C \sum_{n=0}^{N-1} \left\| \rho^{p,n,\theta} \right\|^2 \Delta t$$
$$\leq C(T, \mathbf{u}, p, \mathbf{K}) \left(h^2 + h + \Delta t^{2r} \right).$$

where

$$r = \begin{cases} 1, & \text{if} \quad \theta = 1 \\ 2, & \text{if} \quad \theta = 0 \end{cases}$$

We used the fact that $\sum_{n=0}^{N-1} \Delta t g_n \leq CT \sum_{n=0}^{N-1} g_n$, $|\Omega^*| \leq Ch$ and property that is given in Eq. (33). This finishes the proof of theorem. □

The auxiliary error estimates theorem allows us to conclude the following theorem:

Theorem 2 (*Error Estimate*)**.** *Assume the same conditions as in the previous theorem. Then,*

$$\|p - p_h\|^2_{l^\infty(L^2)} + \|\mathbf{u} - \mathbf{u}_h\|^2_{l^2(L^2)} \leq C \left(h^2 + h + \Delta t^{2r} \right) \tag{47}$$

where $C = C(T, \mathbf{K}, \mathbf{u}, p)$ *and*

$$r = \begin{cases} 1, & \text{if} \quad \theta = 1 \\ 2, & \text{if} \quad \theta = 0 \end{cases}$$

Proof. By applying triangle inequality, the Interpolation Error Inequalities and Theorem 1 results we obtain:

$$\|p - p_h\|^2_{l^\infty(L^2)} + \|\mathbf{u} - \mathbf{u}_h\|^2_{l^2(L^2)} = \left\| E_p^I + E_p^A \right\|^2_{l^\infty(L^2)} + \left\| E_{\mathbf{u}}^I + E_{\mathbf{u}}^A \right\|^2_{l^2(L^2)} \leq$$
$$\leq C \left(\underbrace{\left\| E_p^I \right\|^2_{l^\infty(L^2)} + \left\| E_{\mathbf{u}}^I \right\|^2_{l^2(L^2)}}_{\text{Interpolation error}} + \underbrace{\left\| E_p^A \right\|^2_{l^\infty(L^2)} + \left\| E_{\mathbf{u}}^A \right\|^2_{l^2(L^2)}}_{\text{Auxiliary error}} \right) \leq$$
$$\leq C(T, p, \mathbf{u}, \mathbf{K})(h^2 + h) + O(\Delta t^{2r}) \quad \square$$

4. Numerical examples

In this section, we conduct numerical experiment to verify the numerical accuracy of the transient problem solution using EVMFEM in space and the backward Euler in time. Based on our a *priori* error analysis estimates we assume a

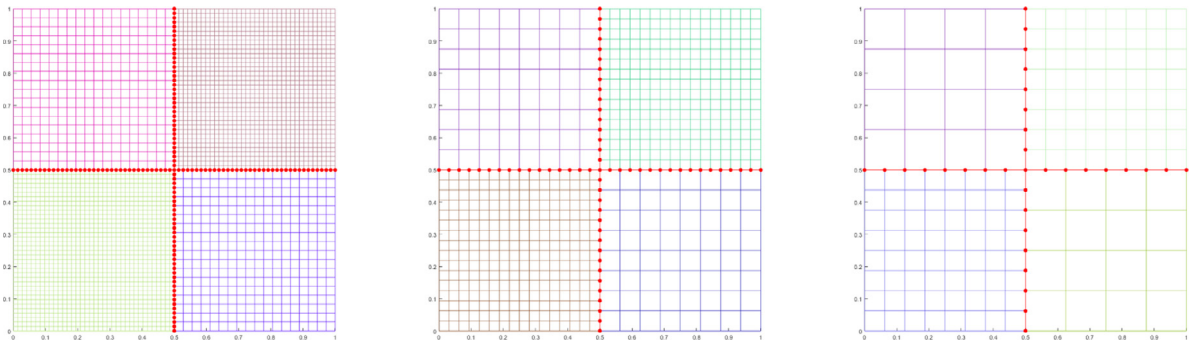

Fig. 4.1. Example of non-matching grids for subdomains.

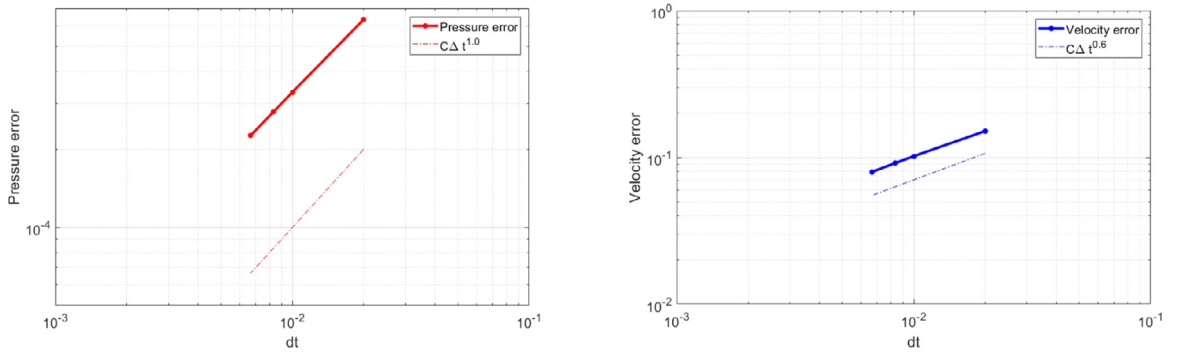

Fig. 4.2. Convergence of the pressure and velocity error.

Table 1
Accuracy results of pressure and velocity for various levels.

Level	h	H	Δt	$error_p$	$error_{\mathbf{u}}$
1	1/52	1/26	1/50	6.33e−04	1.51e−01
2	1/100	1/50	1/100	3.32e−04	1.02e−01
3	1/120	1/60	1/120	2.79e−04	9.15e−02
4	1/152	1/76	1/150	2.26e−04	7.97e−02

sufficiently smooth analytical solution. In numerical examples, we set $\Omega = (0, 1) \times (0, 1)$, $\mathbf{K}_{i,j} = \delta_{i,j}$ and the domain Ω is divided into four subdomains Ω_i; Ω_1 and Ω_4 have fine grids, Ω_2 and Ω_3 have coarse grids; such mesh discretization is illustrated in Fig. 4.1.

4.1. Numerical example 1

We use the known solution

$$p(x, y, t) = tx(1 - x)y(1 - y)$$

and use it to compute the forcing f, the Dirichlet boundary data g, and the initial data p_0. We carry out several levels of uniform grid refinement in each subdomains. The time step and the element size are almost equal to each other, see Table 1. The simulation time interval is $(0; 0.1)$, i.e. $T = 0.1$, and we use the Backward Euler method to integrate with regard to time with uniform time step. We are interested in finding the exact error using a given true solution, so the pressure is true error and the velocity error is normalized error. On applying sufficient Newton iterations at each time step provided the residual is within the machine-precision tolerance, we obtain the numerical solution for evaluating of the error in specified norm. We compute $error_p$, corresponds to $\|p - p_h\|_{l^\infty(L^2)}$, which is maximum of values among time steps that resulting for given time step a discrete pressure L^2-norm that associates only the function values at the cell-centers in space. Also, $error_u$ is defined as $\|\mathbf{u} - \mathbf{u}_h\|_{l^2(L^2)}$ where in space a discrete L^2-norm that associates only the normal vector components at the midpoint edges and then normalized by $\|\mathbf{u}\|_{L^2}$ and l^2-norm in time. The convergence rate is illustrated in Fig. 4.2.

Table 2
Accuracy results of pressure and velocity for various levels.

Level	h	H	Δt	$error_p$	$error_{\mathbf{u}}$
1	1/100	1/50	1/7	7.28e−01	8.64e−01
2	1/128	1/64	1/8	6.38e−01	7.71e−01
3	1/164	1/82	1/9	5.69e−01	6.87e−01
4	1/200	1/100	1/10	5.13e−01	6.24e−01

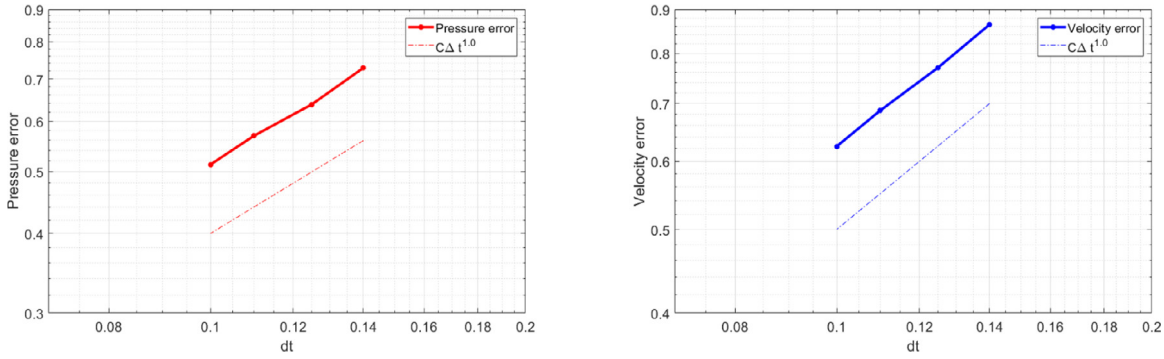

Fig. 4.3. Convergence of pressure and velocity error.

4.2. Numerical example 2

We use the known solution

$$p(x, y, t) = e^t \sin(2\pi x) \sin(2\pi y)$$

and use it to compute the forcing f, the Dirichlet boundary data g, and the initial data p_0. The time step is equal to the root of the coarse mesh size. Thus first order convergence is expected from theoretical result. Such mesh discretization is depicted in Fig. 4.1. The simulation time interval is $(0, 2)$, i.e. $T = 2$, and we use the Backward Euler method to integrate with regard to time with uniform time step, see Table 2. The convergence rate is illustrated in Fig. 4.3.

5. Conclusion

This research has provided a *priori* error analysis for transient problems or slightly compressible flow problems through the heterogeneous porous media using Enhanced Velocity scheme as the domain decomposition method in space that coupled with backward Euler or Crank–Nicolson method in the time setting. In these discretization settings, we obtained the first order convergence rate for the backward Euler method and the second order convergence rate for the Crank–Nicolson method. Numerical tests are provided for validating the backward Euler theory. The results suggest that this approaches could also be useful for the engineering subsurface applications including CO_2 sequestration, etc. In our future research, we plan to concentrate on parareal algorithms to achieve efficiency in time discretization that allow to run simulation efficiently for the long time range.

Acknowledgments

First author thanks Drs. T. Arbogast and I. Yotov for some helpful discussions during analysis of method. First author would like to acknowledge support of the Faculty development Competitive Research Grant (Grant No. 110119FD4502), Nazarbayev University (Kazakhstan).

References

[1] Y. Amanbek, G. Singh, M.F. Wheeler, H. van Duijn, Adaptive numerical homogenization for upscaling single phase flow and transport, J. Comput. Phys. 387 (2019) 117–133.
[2] G. Singh, Y. Amanbek, M.F. Wheeler, Adaptive homogenization for upscaling heterogeneous porous medium, in: SPE Annual Technical Conference and Exhibition, Society of Petroleum Engineers, 2017.
[3] J.A. Wheeler, M.F. Wheeler, I. Yotov, Enhanced velocity mixed finite element methods for flow in multiblock domains, Comput. Geosci. 6 (3-4).
[4] S.G. Thomas, M.F. Wheeler, Enhanced velocity mixed finite element methods for modeling coupled flow and transport on non-matching multiblock grids, Comput. Geosci. 15 (4) (2011) 605–625.
[5] B. Ganis, G. Pencheva, M.F. Wheeler, Adaptive mesh refinement with an enhanced velocity mixed finite element method on semi-structured grids using a fully coupled solver, Comput. Geosci. (2018) 1–20.

[6] Y. Amanbek, A new adaptive modeling of flow and transport in porous media using an enhanced velocity scheme (Ph.D. thesis), 2018.
[7] G. Singh, M.F. Wheeler, A space time domain decomposition approach using enhanced velocity mixed finite element method, arXiv preprint arXiv:1802.05137.
[8] G. Singh, M.F. Wheeler, A domain decomposition approach for local mesh refinement in space and time, arXiv preprint arXiv:1806.10187.
[9] Y. Amanbek, G. Singh, M.F. Wheeler, Selective time-stepping adaptivity for non-linear reactive transport problems, 2017, http://dx.doi.org/10.6084/m9.figshare.4702549.v4.
[10] V. Thomée, Galerkin Finite Element Methods for Parabolic Problems, vol. 1054, Springer, 1984.
[11] M.F. Wheeler, A priori l_2 error estimates for galerkin approximations to parabolic partial differential equations, SIAM J. Numer. Anal. 10 (4) (1973) 723–759.
[12] D.W. Peaceman, Interpretation of well-block pressures in numerical reservoir simulation with nonsquare grid blocks and anisotropic permeability, Soc. Pet. Eng. J. 23 (03) (1983) 531–543.
[13] T. Arbogast, G. Pencheva, M.F. Wheeler, I. Yotov, A multiscale mortar mixed finite element method, Multiscale Model. Simul. 6 (1) (2007) 319–346.
[14] B. Rivière, M.F. Wheeler, A discontinuous galerkin method applied to nonlinear parabolic equations, in: Discontinuous Galerkin Methods, Springer, 2000, pp. 231–244.
[15] T.F. Russell, M.F. Wheeler, Finite Element and Finite Difference Methods for Continuous Flows in Porous Media, SIAM, 1983, pp. 35–106.